

# Saturating a Fundamental Bound on Quantum Measurements' Accuracy

Nicolò Piccione,<sup>1,2,3,\*</sup> Maria Maffei,<sup>4</sup> Andrew N. Jordan,<sup>5,6,7</sup> Kater W. Murch,<sup>8</sup> and Alexia Auffèves<sup>1,2,3</sup>

<sup>1</sup>Université Grenoble Alpes, CNRS, Grenoble INP, Institut Néel, 38000 Grenoble, France

<sup>2</sup>MajuLab, CNRS–UCA–SU–NUS–NTU International Joint Research Laboratory

<sup>3</sup>Centre for Quantum Technologies, National University of Singapore, 117543 Singapore, Singapore

<sup>4</sup>Dipartimento di Fisica, Università di Bari, I-70126 Bari, Italy

<sup>5</sup>The Kennedy Chair in Physics, Chapman University, Orange, CA 92866, USA

<sup>6</sup>Institute for Quantum Studies, Chapman University, Orange, California 92866, USA

<sup>7</sup>Department of Physics and Astronomy, University of Rochester, Rochester, New York 14627, USA

<sup>8</sup>Department of Physics, Washington University, St. Louis, Missouri 63130, USA

A quantum system is usually measured through observations performed on a second quantum system, or meter, to which it is coupled. In this scenario, fundamental limitations arise as stated by the celebrated Wigner-Araki-Yanase theorem and its generalizations, predicting an upper-bound on the measurement's accuracy (Ozawa's bound). Here, we show it is possible to saturate this fundamental bound. We propose a simple interferometric setup, arguably within reach of present technology, in which a flying particle (the quantum meter) is used to measure the state of a qubit (the target system). We show that the bound can be saturated and that this happens only if the flying particle is prepared in a Gaussian wavepacket.

According to von Neumann's prescription [1], a quantum measurement starts with a *pre-measurement* [1], i.e., an interaction between the measured system and a second system called a *quantum meter* which is then collapsed by a classical apparatus. For example, in a Stern-Gerlach experiment, the particles' spin is measured by mapping it onto their position that is then observed on a detector screen. The celebrated Wigner-Araki-Yanase (WAY) theorem [2–4] and its generalizations [5–11] pose limits on the accuracy of quantum measurements. In particular, Ozawa [5] derived an expression for their minimal inaccuracy, often dubbed Ozawa's bound. Nevertheless, previous to this work, the strictness of this bound has not been proved, and no example of a dynamics saturating this bound is known.

One natural scenario for the application of the WAY theorem and Ozawa's bound can be found within scattering-type measurement dynamics [12, 13]. In such dynamics, the system is autonomous (i.e., the system-meter Hamiltonian is time-independent) and the interaction between meter and system is negligible at the initial and final times of the considered dynamics<sup>1</sup>. Limitations to the accuracy of quantum measurements in this physical situation arise whenever the system observable one wants to measure does not commute with the system Hamiltonian. In this scenario, Ozawa's bound depends on the energy dispersions of the system and meter respectively. The regime of ideal measurement corresponds to a vanishing bound. It is reached when the meter's energy dispersion is much larger than the system's energy scale, making the energy change of the meter hardly de-

tectable. This measurement gives rise to energy variations of the system's energy which have been called *quantum heat* [14–16] or *measurement energy* [17]. Remarkably, Ozawa's bound has never been saturated. Whether it can be saturated in a scattering-type measurement and under which conditions remain open questions.

In this letter, we consider a scattering-type pre-measurement based on a feasible interferometric scheme. In the considered setting, the quantum meter is a flying particle and the system to measure, or target system, is a qubit. The interferometer allows measurement of the qubit's state along the  $z$ -axis by using the flying particle position as a pointer. By tilting the qubit's Hamiltonian with respect to the  $z$ -axis, we study the situation considered by Ozawa where the system's bare Hamiltonian does not commute with the measurement observable. Contrary to the general case, Ozawa's bound does not depend on the initial state of the qubit, but only on that of the flying particle. Most importantly, we show that the bound can be saturated, and this happens if and only if the flying particle (i.e., the meter) is prepared in a Gaussian wavepacket. To the best of our knowledge, the implementation of our scheme or a similar one would provide the first experimental test of the strictness of Ozawa's bound. This test can be implemented within state-of-the-art architectures of waveguide quantum photonics, superconducting circuits, and atomic physics.

*Ozawa's bound:* Let us consider a target system  $S$  interacting with a meter system  $M$  within joint unitary dynamics described by the unitary operator  $U$ . We will denote by  $O_S$  the observable we wish to measure on  $S$ , and with  $O_M$  the pointer observable, i.e., the observable of  $M$  to be measured via a classical apparatus to readout the value of  $O_S$ . Finally, let  $L_S$  and  $L_M$  be two Hermitian operators acting respectively on  $S$  and  $M$  such that their sum is a conserved quantity, i.e.,  $[L_S + L_M, U] = 0$ . Fol-

<sup>1</sup> Moreover, the effective duration of the interaction between meter and system is given by the amount of time their wavefunctions overlap non-negligibly.

lowing Ref. [5], we define a noise operator  $N = U^\dagger O_M U - O_S$  giving the readout error (or measurement's inaccuracy)  $\varepsilon^2(|\psi_S\rangle) = \langle \psi_S, \psi_M | N^2 | \psi_S, \psi_M \rangle$ , where  $|\psi_S\rangle$  and  $|\psi_M\rangle$  are, respectively, the states of system and meter before the interaction ( $t = t_0$ ). Assuming  $[L_M, O_M] = 0$ , (the so-called Yanase's condition [8]) Ozawa derived the following bound for the error:

$$\varepsilon^2(|\psi_S\rangle) \geq \varepsilon_B^2(|\psi_S\rangle) = \frac{1}{4} \frac{|\langle \psi_S | [O_S, L_S] | \psi_S \rangle|^2}{\Delta L_S^2 + \Delta L_M^2}, \quad (1)$$

where the variance  $\Delta L_S^2 = \langle L_S^2 \rangle - \langle L_S \rangle^2$  is computed on the initial state of  $S$  and similarly for  $\Delta L_M^2$ . Remarkably, the bound does not depend on the interaction between system and meter nor on the pointer observable  $O_M$ . The initial state of the meter  $M$  only enters the bound through the variance  $\Delta L_M$ . In agreement with the WAY statement, the bound goes to zero when  $\Delta L_M \rightarrow \infty$ . Hence, for all practical purposes, we recover that Ozawa's bound is negligible when macroscopic meters are employed.

*Measurement setup:* We consider a measurement scheme where  $S$  is a qubit,  $M$  is a flying particle, and the classical measurement apparatus is a Mach-Zehnder interferometer, as depicted in Fig. 1. We denote the eigenstates of the qubit along the  $z$ -axis by  $|g_z\rangle$  and  $|e_z\rangle$  which are, respectively, the ground and excited state. The qubit can be fixed in space (as in Fig. 1) or be attached to the flying particle (being a so-called internal degree of freedom). More details on possible experimental realizations will be given later in the paper.

The qubit's Hamiltonian is  $H_S = (\hbar\omega_q/2)[\cos(\Theta)\sigma_z + \sin(\Theta)\sigma_x]$  where  $\omega_q$  is its bare frequency,  $\Theta$  is an angle that can vary in  $[0, \pi/2]$ ,  $\sigma_x = |g_z\rangle\langle e_z| + |e_z\rangle\langle g_z|$  and  $\sigma_z = |g_z\rangle\langle g_z| - |e_z\rangle\langle e_z|$  are Pauli matrices. The Hamiltonian of the flying particle is  $H_M = v_0\hat{p}$ , where  $v_0$  is its group velocity.  $H_M$  is the so-called quantum clock Hamiltonian [18–24], which can be derived from the usual particle Hamiltonian  $\hat{p}^2/2m$  under certain conditions [24]. Using  $H_M$  corresponds to linearizing the kinetic energy in solid-state physics (used for flying qubits in [24, 25]). Moreover,  $H_M$  can also be seen as the Hamiltonian of a single photon propagating in a one-dimensional path with a linear dispersion relation [26, 27]. At  $t = t_0 < 0$ , prior to the beginning of the interaction, the meter's state is described by the wavepacket  $\psi_0(x)$ , with a spatial spread  $\Delta x^2 \equiv \int_{-\infty}^{+\infty} (x - x_0)^2 |\psi_0(x)|^2 dx$ , where  $x_0 = v_0 t_0$  is the wavepacket's average position at the initial time  $t_0$ . Finally, the Hamiltonian governing the system-meter dynamics is

$$H = H_M + H_S + \frac{\hbar\phi v_0}{2} \delta(\hat{x}) \otimes \sigma_z, \quad (2)$$

where  $\delta(\hat{x})$  indicates that we consider a qubit whose position is fixed at  $x = 0$ , and  $\phi \in [0, 2\pi]$  is an angle char-

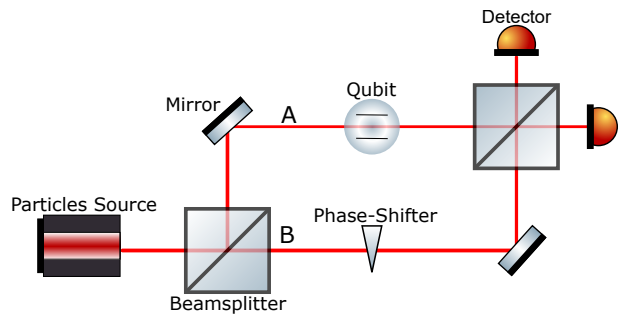


FIG. 1. Setup of the proposed measurement scheme, based on a Mach-Zehnder interferometer. A flying particle (the meter) passes through a balanced beamsplitter. In path  $A$  it interacts with the qubit, in path  $B$  it always acquires the same phase  $\pi/2$ . The two paths then recombine by means of a second balanced beamsplitter. In the case of an ideal projective measurement of  $\sigma_z$ , corresponding to  $\{\Theta, \phi\} = \{0, \pi\}$ , the particle is found with certainty by the upper detector if the qubit state is  $|g_z\rangle$  and by the other one if it is  $|e_z\rangle$ .

acterizing the strength of the pre-measurement. In the standard case where  $H_S \propto \sigma_z$ ,  $\phi/2$  represents the phase shift acquired by the flying particle as a result of the interaction with the qubit, **independently of  $v_0$** . Since the wavepacket moves at constant velocity without deformation [24], the effective duration of the pre-measurement interaction reads  $\Delta t = \Delta x/v_0$  and the wavepacket's average position is at qubit's position ( $x = 0$ ) when  $t = 0$ . Upon defining the wavepacket's frequency operator  $\hat{\omega} \equiv (v_0/\hbar)\hat{p}$ , we find that the wavepacket satisfies the time-frequency Heisenberg's uncertainty relation  $\Delta\omega\Delta t \geq 1/2$ .

The setup measures the qubit observable  $O_S = \sigma_z$  as follows: the flying particle goes through a first beam splitter which generates a balanced superposition between the output paths  $A$  and  $B$ . The interaction with the target qubit takes place in the arm  $A$ , while the arm  $B$  contains a phase shifter introducing a phase of  $\pi/2$ . Finally, the second balanced beam-splitter recombines the two paths and then a classical measurement finds out whether the particle is in path  $A$  or  $B$ , performing the qubit's readout.

Let us illustrate the working principle of the setting in the simplest case, where it achieves an ideal projective measurement of  $\sigma_z$ . This case corresponds to taking two assumptions:  $\Theta = 0$ , and  $\phi = \pi$ . The latter assumption is known in quantum optics as the  $\pi$ -per-photon condition. Under these assumptions, the flying particle acquires a phase of  $e^{\pm i\pi/2}$  depending on the qubit state along  $\sigma_z$ . At the output of the second balanced beam splitter, the particle is found in path  $A$  if the qubit was in  $|e_z\rangle$ , and in path  $B$  if the qubit was in  $|g_z\rangle$ . Finally, we define the pointer observable as  $O_M = \hat{n}_A - \hat{n}_B$ , where  $\hat{n}_A$  measures if the particle is in  $A$  with outcomes 0 (no particle) and 1 (there is a particle) and  $\hat{n}_B$  does the same

for path  $B$ . The WAY theorem's assumptions are satisfied upon the identification  $L_S = H_S$  and  $L_M = H_M$  because beamsplitters are energy conserving at the scattering level<sup>2</sup> and the particle-qubit interaction is of the scattering type [12] thus implying  $[H_S + H_M, U] = 0$ , where the unitary operator  $U$  describes the entire pre-measurement dynamics (beamsplitters included).

*Results:* Now, we consider the case where the qubit's Hamiltonian  $H_S$  is tilted by an angle  $\Theta \in (0, \pi/2]$  so that  $[H_S, \sigma_z] \neq 0$ . Because of this non-commutation, the observable  $\sigma_z$ , in the interaction picture, changes in time due to the qubit's bare Hamiltonian. For an ideal projective measurement, we would have to clearly define at what time we instantaneously measure the observable. However, in our case, the measurement takes a finite amount of time. Therefore, for definiteness, we consider the goal of our setup to measure  $\sigma_z$  as it was at the initial time  $t = t_0$ . Hereafter, we also relax the condition on the phase acquired by the flying particle, considering also the cases where the angle  $\phi$  is different from  $\pi$ . However, we will see that the best accuracy is always attained for  $\phi = \pi$ .

Let us write the qubit's state at  $t = t_0$  as  $|\psi_S\rangle = b_g |g_\Theta\rangle + b_e |e_\Theta\rangle$ , where  $|g_\Theta\rangle$  and  $|e_\Theta\rangle$  are, respectively, the ground and excited states of  $H_S$ . In the SM [28], we show that the interaction between the particle and the qubit (in the interaction picture) leads to the map:

$$|\psi_S, 1_\omega\rangle \rightarrow b_g I_{gg} |g_\Theta, 1_\omega\rangle + b_e I_{ee} |e_\Theta, 1_\omega\rangle + b_g I_{ge} |e_\Theta, 1_{\omega-\omega_q}\rangle + b_e I_{eg} |g_\Theta, 1_{\omega+\omega_q}\rangle, \quad (3)$$

where  $I_{gg} = I_{ee}^* = \cos(\phi/2) + i \cos(\Theta) \sin(\phi/2)$ ,  $I_{ge} = I_{eg} = i \sin(\Theta) \sin(\phi/2)$ , and  $|1_\omega\rangle$  is the starting meter's state, whose average frequency is  $\omega$ . As shown in the SM [28], the particle's wavefunctions  $|1_{\omega \pm \omega_q}\rangle$  are shaped as the input one<sup>3</sup> but shifted in frequency by the qubit's frequency  $\omega_q$ , as expected from energy conservation in scattering processes. The readout error then reads (see the SM [28] for the derivation):

$$\varepsilon^2 = 2 \left\{ 1 - \sin\left(\frac{\phi}{2}\right) [\cos^2(\Theta) + P \sin^2(\Theta)] \right\}, \quad (4)$$

where

$$P \equiv \text{Re}\{\langle 1_\omega | 1_{\omega+\omega_q} \rangle\} = \int dx |\psi_0(x)|^2 \cos\left(\frac{\omega_q(x-x_0)}{v_0}\right). \quad (5)$$

We can see that the highest accuracy is attained for  $\phi = \pi$ , independently of  $\Theta$ . Hence, setting  $\phi = \pi$  we can write

$$\varepsilon = \sin(\Theta) \sqrt{2(1-P)}. \quad (6)$$

<sup>2</sup> In other words, the energy of the particle before and after the interaction with the beam-splitter is the same.

<sup>3</sup> That is,  $|\langle x | 1_{\omega \pm \omega_q} \rangle|^2 = |\langle x | 1_\omega \rangle|^2$ .

Indeed, perfect accuracy ( $\varepsilon = 0$ ) is attained in the full commuting case  $\Theta = 0$ . Alternatively, for any  $\Theta$ , it can be attained for  $P \rightarrow 1$ , which entails that the shifted meter's wavepackets are completely indistinguishable from the input one. This ideal situation is consistent with an infinite frequency dispersion of the meter's initial state.

*Ozawa's bound:* We now compare the readout error displayed on Eq. (6) to the fundamental bound derived by Ozawa [see Eq. (1)]. Remarkably, the error given in Eq. (4) is independent of the initial qubit's state. Therefore, it can be compared with Ozawa's bound [Eq. (1)] maximized over all possible initial qubit states. This can be done as follows: first, we notice that  $[\sigma_z, H_S] = i\hbar\omega_q \sin(\Theta)\sigma_y$  and inserting it into Eq. (1), upon defining  $\sigma_\Theta \equiv \cos(\Theta)\sigma_z + \sin(\Theta)\sigma_x$ , one gets

$$\varepsilon_B^2(|\psi_S\rangle) = \frac{\sin^2(\Theta) \langle \sigma_y \rangle^2}{1 + 4(\Delta\omega/\omega_q)^2 - \langle \sigma_\Theta \rangle^2}. \quad (7)$$

In the above equation, we have used that  $\Delta H_M = \hbar\Delta\omega$ , with  $\Delta\omega$  being the frequency dispersion of the flying particle. For a fixed value of  $\langle \sigma_y \rangle$ , the goal is to maximize  $\langle \sigma_\Theta \rangle^2$ <sup>4</sup>. When this is done, we obtain that  $\langle \sigma_\Theta \rangle^2 + \langle \sigma_y \rangle^2 = 1$ , yielding

$$\varepsilon_B^2(|\psi_S\rangle) = \max_{\langle \sigma_y \rangle} \frac{\sin^2(\Theta) \langle \sigma_y \rangle^2}{4(\Delta\omega/\omega_q)^2 + \langle \sigma_y \rangle^2} = \frac{\sin^2(\Theta)}{1 + 4(\Delta\omega/\omega_q)^2}, \quad (8)$$

where the maximum is attained by choosing  $\langle \sigma_y \rangle = \pm 1$ , which implies  $\langle \sigma_\Theta \rangle = 0$ .

For any  $\Theta$ ,  $\varepsilon_B \ll 1$  when  $\Delta\omega \gg \omega_q$ . This can be understood by considering Eq. (3) which shows that the flying particle's states after the interaction are shifted in frequency of  $\pm\omega_q$ . Then, the less visible the frequency shift undergone by the flying particle, the more accurate the readout can be. Note that however, the meter's frequency shift can be observed by means of post-selection, for sufficiently small tilts  $\Theta \rightarrow 0$  [23]. In the opposite regime,  $\Delta\omega \ll \omega_q$ , the meter carries information on the qubit energy state and its energy shifts can be used to access quantum heat exchanges, as done in Ref. [16].

*Saturation of the bound in the short interaction regime:* Up to now, we analyzed the pre-measurement scheme in great generality. We obtained the general formula for the error as defined by Ozawa [Eq. (4)] and the fundamental bound derived by Ozawa [Eq. (8)] in a form specific to our model. We now explore under which conditions Eq. (4) can practically reduce to Eq. (8), i.e.,

<sup>4</sup> Splitting the maximization in two steps poses no problems because for such simple sets it holds the following: the maximum of the set of maxima of subsets covering the starting set is also the maximum of the entire set. For the same reason, the order of the two maximizations does not matter

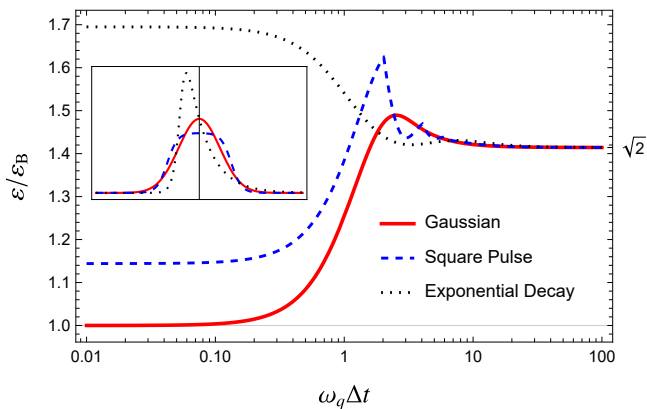


FIG. 2. Ratio  $\varepsilon/\varepsilon_B$  as a function of  $\omega_q \Delta t$  for different wavepacket shapes. The inset in the top-left corner show the three shapes: Gaussian, square pulse, exponential decay. As predicted, only the Gaussian wavepacket saturates Ozawa's bound for  $\omega_q \Delta t \ll 1$ . In other regimes, the best shape is not the Gaussian anymore. Moreover, for every shape, we get  $\varepsilon/\varepsilon_B = \sqrt{2}$  for  $\omega_q \Delta t \gg 1$ .

the conditions for which we can saturate Ozawa's bound ( $\varepsilon \geq \varepsilon_B \rightarrow \varepsilon = \varepsilon_B$ ). To do so, we set  $\phi = \pi$  and we analyze the regime in which  $\omega_q \Delta t \ll 1$ , which implies  $\Delta\omega \gg \omega_q$  due to Heisenberg's uncertainty principle ( $\Delta\omega \Delta t \geq 1/2$ ). In other words, the interaction time between meter and qubit is much shorter than  $1/\omega_q$ . This is the regime in which, despite having  $\Theta > 0$ , accurate measurements of  $\sigma_z$  can be attained and thus the one of most practical importance.

In this regime, Ozawa's bound [Eq. (8)] can be approximated to  $\varepsilon_B \simeq \sin(\Theta)\omega_q/(2\Delta\omega)$ , Eq. (5) to  $P \simeq 1 - (1/2)\omega_q^2 \Delta t^2$ , and the error reads [cf. Eq. (6)]  $\varepsilon \simeq \sin(\Theta)\omega_q \Delta t$ . Therefore, when the initial state of the flying particle satisfies the minimum uncertainty relation  $\Delta\omega \Delta t = 1/2$ , we get  $\varepsilon \simeq \varepsilon_B$ . In other words, in the short interaction regime, Ozawa's bound can be practically saturated, but only by Gaussian wavepackets, the only wavepackets satisfying the minimum uncertainty relation [29]. For longer interaction times, the bound is not saturated anymore. In particular, for  $P \rightarrow 0$ , attained for  $\Delta\omega \ll \omega_q$ , the ratio of error and bounds gives  $\varepsilon/\varepsilon_B = \sqrt{2}$ . This corresponds to the regime in which the energies of qubit and meter are strongly correlated.

All previous considerations are exemplified in Fig. 2, where we plotted the ratio  $\varepsilon/\varepsilon_B$  as a function of  $\omega_q \Delta t$  for different wavepacket shapes. We can see that, indeed, only the Gaussian wavepacket saturates Ozawa's Bound. More details on how these plots have been obtained can be found in Sec. III of the SM [28].

*Possible experimental implementations:* The setup of Fig. 1, or an equivalent one, can be implemented in various physical platforms. Options include circuit QED, quantum photonics, and flying particles with internal de-

grees of freedom (IDoF). Among these possibilities, the most-promising one appears to us the one implementable in circuit QED settings. We will first briefly comment on the last two and then, more in detail, on the first one.

Regarding flying particles, our scheme could be implemented by treating their IDoF [24] as the qubit to measure. A spatially localized field acting on the IDoF can implement the system-meter interaction. Moreover, if there is no energy difference between the IDoF states, a global field can be used to implement  $H_S$ . Notice that beamsplitters for massive particles such as electrons [30], atoms [31–37], and molecules [32, 35, 36] are actively investigated.

In quantum photonics, a single-photon wavepacket can play the meter role and the qubit states could be encoded in two possible propagation paths. By making these paths close enough, the photon can hop among them during the propagation, thus implementing an Hamiltonian  $H_S \propto \sigma_x$  [38–40] whose magnitude can be much smaller than the photon energy (as in Ref. [38]) while the scattering-type interaction  $\delta(\hat{x}) \otimes \sigma_z$  of Eq. (2) could be implemented by inserting two different refractive materials in the two paths.

In circuit QED, dispersive interactions followed by interferometric readouts are widely used to measure superconducting (transmon) qubits in microwave resonators [41, 42]. The Hamiltonian  $H_S$  with  $\Theta \neq 0$  can be implemented by driving the qubit with a classical field [16, 42–46] while the meter Hamiltonian can be obtained by considering a single photon traveling in the waveguide [26, 27]. In Ref. [16], a qubit Hamiltonian with  $\Theta = \pi/2$  has been implemented in this way, with a frequency  $\omega_q \sim 1$  MHz. The natural qubit Hamiltonian along the  $z$ -axis, with frequency  $\omega_z \sim$  GHz, is eliminated by studying the dynamics in the rotating frame with the same frequency. In this case, the central frequency of the traveling photon is around  $\omega \sim 5$  GHz so that its frequency dispersion can well be  $\Delta\omega \sim 10$  MHz so that  $\omega \gg \Delta\omega \gg \omega_q$ , thus making the good-measurement regime physically allowed. The experimental measurement of the readout error as defined by Ozawa requires separate access to the measurements of  $O_M$  and  $O_S$ , which is easily achievable in this kind of platform. Finally, pulse-shaping techniques can be used to make various types of one-photon wavepackets as in Fig. 2.

*Conclusions and outlooks:* We proposed an interferometric scheme allowing one to saturate a fundamental bound on the accuracy of scattering-type quantum measurements, hence showing that the bound is strict. In particular, we showed that, in our setup, the saturation can be attained only if the quantum meter, a flying particle, is prepared in a Gaussian wavepacket. Finally, we argued how our scheme could be experimentally implemented, allowing for a first experimental test of Ozawa's bound.

Recent experimental progresses is pushing the fundamental bounds of measurements (see for example [47]). In this regard, our work paves the way to an experiment whose aim is to test Ozawa's fundamental bound. Moreover, the accuracy bound saturated in this letter as well as other fundamental bounds investigated in the literature have practical consequences for quantum technologies. Although macroscopic meters make them negligible, this is not so when quantum meters (sometimes called ancillas) are used [13, 48]. In fact, while increasing the size of the meter can increase the accuracy of the measurement, it can also greatly increase the practical energetic cost of the measurement operation [49, 50]. Therefore, measurement schemes saturating these bounds can be of great importance for the energetic cost of quantum technologies [51].

*Acknowledgements.*—This work was supported by the Foundational Questions Institute Fund (Grant No. FQXi-IAF19-01 and Grant No. FQXi-IAF19-05), the John Templeton Foundation (Grant No. 61835), the ANR Research Collaborative Project “Qu-DICE” (Grant No. ANR-PRC-CES47), and the National Research Foundation, Singapore and A\*STAR under its CQT Bridging Grant. M. M. acknowledges the support by PNR MUR project PE0000023-NQSTI.

We thank M. Richard and R. Whitney for useful discussions about possible experiments to verify our results. N.P. thanks R. Takagi and H. Wilming, for useful discussions about the results of this work.

---

\* [nicolo'.piccione@units.it](mailto:nicolo.piccione@units.it)

- [1] A. N. Jordan and I. A. Siddiqi, *Quantum Measurement: Theory and Practice* (Cambridge University Press, 2024).
- [2] P. Busch, Translation of "Die Messung quantenmechanischer Operatoren" by E.P. Wigner, [arXiv:1012.4372](https://arxiv.org/abs/1012.4372) (2010).
- [3] H. Araki and M. M. Yanase, Measurement of quantum mechanical operators, *Phys. Rev.* **120**, 622 (1960).
- [4] M. M. Yanase, Optimal measuring apparatus, *Phys. Rev.* **123**, 666 (1961).
- [5] M. Ozawa, Conservation laws, uncertainty relations, and quantum limits of measurements, *Phys. Rev. Lett.* **88**, 050402 (2002).
- [6] S. Luo, Wigner-yanase skew information and uncertainty relations, *Phys. Rev. Lett.* **91**, 180403 (2003).
- [7] T. Miyadera and H. Imai, Wigner-araki-yanase theorem on distinguishability, *Phys. Rev. A* **74**, 024101 (2006).
- [8] L. Loveridge and P. Busch, ‘measurement of quantum mechanical operators’ revisited, *The European Physical Journal D* **62**, 297 (2011).
- [9] M. Navascués and S. Popescu, How energy conservation limits our measurements, *Phys. Rev. Lett.* **112**, 140502 (2014).
- [10] Y. Kuramochi and H. Tajima, Wigner-araki-yanase theorem for continuous and unbounded conserved observables, [arXiv:2208.13494](https://arxiv.org/abs/2208.13494) (2022).
- [11] H. Tajima, R. Takagi, and Y. Kuramochi, *Universal trade-off structure between symmetry, irreversibility, and quantum coherence in quantum processes* (2022).
- [12] J. R. Taylor, *Scattering theory: the quantum theory of nonrelativistic collisions* (Courier Corporation, 2006).
- [13] R. Katsube, M. Ozawa, and M. Hotta, Limitations of quantum measurements and operations of scattering type under the energy conservation law, [arXiv:2211.13433](https://arxiv.org/abs/2211.13433) (2023).
- [14] C. Elouard, D. A. Herrera-Martí, M. Clusel, and A. Auffèves, The role of quantum measurement in stochastic thermodynamics, *npj Quantum Information* **3**, 1 (2017).
- [15] L. Bresque, P. A. Camati, S. Rogers, K. Murch, A. N. Jordan, and A. Auffèves, Two-qubit engine fueled by entanglement and local measurements, *Phys. Rev. Lett.* **126**, 120605 (2021).
- [16] X. Linpeng, N. Piccione, M. Maffei, L. Bresque, S. P. Prasad, A. N. Jordan, A. Auffèves, and K. W. Murch, Quantum energetics of a non-commuting measurement, [arXiv:2311.13634](https://arxiv.org/abs/2311.13634) (2023).
- [17] S. Rogers and A. N. Jordan, Postselection and quantum energetics, *Phys. Rev. A* **106**, 052214 (2022).
- [18] Y. Aharonov and T. Kaufherr, Quantum frames of reference, *Phys. Rev. D* **30**, 368 (1984).
- [19] Y. Aharonov, J. Oppenheim, S. Popescu, B. Reznik, and W. G. Unruh, Measurement of time of arrival in quantum mechanics, *Phys. Rev. A* **57**, 4130 (1998).
- [20] A. S. Malabarba, A. J. Short, and P. Kammerlander, Clock-driven quantum thermal engines, *New Journal of Physics* **17**, 045027 (2015).
- [21] N. Gisin and E. Zambrini Cruzeiro, Quantum measurements, energy conservation and quantum clocks, *Annalen der Physik* **530**, 1700388 (2018).
- [22] S. Sołtan, M. Frączak, W. Belzig, and A. Bednorz, Conservation laws in quantum noninvasive measurements, *Phys. Rev. Research* **3**, 013247 (2021).
- [23] S. Rogers and A. N. Jordan, Postselection and quantum energetics, *Phys. Rev. A* **106**, 052214 (2022).
- [24] N. Piccione, L. Bresque, A. N. Jordan, R. S. Whitney, and A. Auffèves, Reservoir-free decoherence in flying qubits, [arXiv:2305.02746](https://arxiv.org/abs/2305.02746) (2023).
- [25] M. Yamamoto, S. Takada, C. Bäuerle, K. Watanabe, A. D. Wieck, and S. Tarucha, Electrical control of a solid-state flying qubit, *Nature Nanotechnology* **7**, 247 (2012).
- [26] J.-T. Shen and S. Fan, Theory of single-photon transport in a single-mode waveguide. i. coupling to a cavity containing a two-level atom, *Phys. Rev. A* **79**, 023837 (2009).
- [27] N. Piccione, M. Maffei, X. Linpeng, A. N. Jordan, K. W. Murch, and A. Auffèves, Fundamental mechanisms of energy exchanges in autonomous measurements based on dispersive qubit-light interaction, [arXiv:2311.11870](https://arxiv.org/abs/2311.11870) (2023).
- [28] See supplemental material at . . . [URL will be inserted by the publisher], (2023).
- [29] C. Cohen-Tannoudji, B. Diu, and F. Laloë, *Quantum Mechanics, Volume 1: Basic Concepts, Tools, and Applications* (John Wiley & Sons, 2019).
- [30] Y. Ji, Y. Chung, D. Sprinzak, M. Heiblum, D. Mahalu, and H. Shtrikman, An electronic mach-zehnder interferometer, *Nature* **422**, 415 (2003).
- [31] R. Huesmann, C. Balzer, P. Courteille, W. Neuhauser, and P. E. Toschek, Single-atom interferometry, *Phys. Rev. Lett.* **82**, 1611 (1999).

- [32] A. D. Cronin, J. Schmiedmayer, and D. E. Pritchard, Optics and interferometry with atoms and molecules, *Rev. Mod. Phys.* **81**, 1051 (2009).
- [33] S. Machluf, Y. Japha, and R. Folman, Coherent Stern–Gerlach momentum splitting on an atom chip, *Nat. Comm.* **4**, 2424 (2013).
- [34] B. Barrett, R. Geiger, I. Dutta, M. Meunier, B. Canuel, A. Gauguet, P. Bouyer, and A. Landragin, The sagnac effect: 20 years of development in matter-wave interferometry, *Comptes Rendus Physique* **15**, 875 (2014), the Sagnac effect: 100 years later / L’effet Sagnac : 100 ans après.
- [35] M. Keil, O. Amit, S. Zhou, D. Groswasser, Y. Japha, and R. Folman, Fifteen years of cold matter on the atom chip: promise, realizations, and prospects, *Journal of modern optics* **63**, 1840 (2016).
- [36] L. Amico, M. Boshier, G. Birkl, A. Minguzzi, C. Miniatura, L.-C. Kwek, D. Aghamalyan, V. Ahufinger, D. Anderson, N. Andrei, *et al.*, Roadmap on atomtronics: State of the art and perspective, *AVS Quantum Science* **3**, 039201 (2021).
- [37] Y. Margalit, O. Dobkowsky, Z. Zhou, O. Amit, Y. Japha, S. Moukouri, D. Rohrich, A. Mazumdar, S. Bose, C. Henkel, *et al.*, Realization of a complete stern-gerlach interferometer: Toward a test of quantum gravity, *Science advances* **7**, eabg2879 (2021).
- [38] A. Peruzzo, M. Lobino, J. C. F. Matthews, N. Matsuda, A. Politi, K. Poulios, X.-Q. Zhou, Y. Lahini, N. Ismail, K. Wörhoff, Y. Bromberg, Y. Silberberg, M. G. Thompson, and J. L. O’Brien, Quantum walks of correlated photons, *Science* **329**, 1500 (2010).
- [39] A. Aspuru-Guzik and P. Walther, Photonic quantum simulators, *Nat. Phys.* **8**, 285 (2012).
- [40] J. Wang, F. Sciarrino, A. Laing, and M. G. e. a. Thompson, Integrated photonic quantum technologies, *Nat. Photonics* **14**, 273 (2020).
- [41] M. H. Devoret and R. J. Schoelkopf, Superconducting circuits for quantum information: An outlook, *Science* **339**, 1169 (2013).
- [42] A. Blais, A. L. Grimsmo, S. M. Girvin, and A. Wallraff, Circuit quantum electrodynamics, *Rev. Mod. Phys.* **93**, 025005 (2021).
- [43] A. Blais, R.-S. Huang, A. Wallraff, S. M. Girvin, and R. J. Schoelkopf, Cavity quantum electrodynamics for superconducting electrical circuits: An architecture for quantum computation, *Phys. Rev. A* **69**, 062320 (2004).
- [44] A. Blais, J. Gambetta, A. Wallraff, D. I. Schuster, S. M. Girvin, M. H. Devoret, and R. J. Schoelkopf, Quantum information processing with circuit quantum electrodynamics, *Phys. Rev. A* **75**, 032329 (2007).
- [45] J. Gambetta, A. Blais, M. Boissonneault, A. A. Houck, D. I. Schuster, and S. M. Girvin, Quantum trajectory approach to circuit qed: Quantum jumps and the zeno effect, *Phys. Rev. A* **77**, 012112 (2008).
- [46] M. Boissonneault, J. M. Gambetta, and A. Blais, Dispersive regime of circuit qed: Photon-dependent qubit dephasing and relaxation rates, *Phys. Rev. A* **79**, 013819 (2009).
- [47] S. Hong, Y.-S. Kim, Y.-W. Cho, J. Kim, S.-W. Lee, and H.-T. Lim, Demonstration of complete information trade-off in quantum measurement, *Phys. Rev. Lett.* **128**, 050401 (2022).
- [48] M. Ozawa, Conservative quantum computing, *Phys. Rev. Lett.* **89**, 057902 (2002).
- [49] M. Fellous-Asiani, J. H. Chai, R. S. Whitney, A. Auffèves, and H. K. Ng, Limitations in quantum computing from resource constraints, *PRX Quantum* **2**, 040335 (2021).
- [50] M. Fellous-Asiani, J. H. Chai, Y. Thonnart, H. K. Ng, R. S. Whitney, and A. Auffèves, Optimizing resource efficiencies for scalable full-stack quantum computers, [arXiv:2209.05469](https://arxiv.org/abs/2209.05469) (2022).
- [51] A. Auffèves, Quantum technologies need a quantum energy initiative, *PRX Quantum* **3**, 020101 (2022).

## Supplemental Material Saturating a Fundamental Bound on Quantum Measurements' Accuracy

### SCATTERING MAP

In this section, we derive Eq. (3) of the main text. The bipartite system we study is composed of the following Hamiltonian:

$$H = H_S + H_M + V, \quad H_S = \frac{\hbar\omega_q}{2} [\cos(\Theta)\sigma_z + \sin(\Theta)\sigma_x], \quad H_M = v_0\hat{q}, \quad V = \frac{\hbar\phi v_0}{2} f(\hat{x})\sigma_z, \quad (\text{S1})$$

where  $f(\hat{x})$  is a generic function of the position operator  $\hat{x}$ . As in the main text, the initial state of the qubit is  $|\psi_S\rangle = b_g |g_\Theta\rangle + b_e |e_\Theta\rangle$ . The initial state of the meter is instead given by  $|1_\omega\rangle$ , representing a wavepacket centered around the frequency  $\omega$ . The frequency, here, corresponds to the wavevector multiplied by  $v_0$ , i.e.,  $\omega = v_0 k$ , where  $k = p/\hbar$  is a wavevector. Notice that, with respect to the main text, here the dynamics starts at  $t = 0$  to lighten the notation. In other words, at  $t = 0$ , the meter's wavepacket is still far on the left of the qubit's position ( $x=0$ ).

Let us denote the initial wavefunction of the meter by  $\psi_M(x)$ . It can be seen<sup>5</sup> that

$$|\psi(t)\rangle = \int_{-\infty}^{+\infty} dx \psi_M(x - v_0 t) U(x + v_0 t; x) |x\rangle |\psi_S\rangle, \quad U(x + v_0 t; x) = \mathcal{T} \exp \left\{ -\frac{i}{\hbar} \int_0^t \left[ H_S + \frac{\hbar\phi v_0}{2} f(x + v_0 s) \sigma_z \right] ds \right\}, \quad (\text{S2})$$

by inserting the above formula into the Schrödinger equation. Let us now consider the limit for which  $f(x) \rightarrow \delta(x)$  and the long-time limit for which  $t$  is always high enough such that  $s = -x/v_0$  is always within the integration extremes. Then, the unitary operator can be written as follows:

$$U(x + v_0 t; x) = e^{-(i/\hbar)(t+x/v_0)H_S} e^{-i(\phi/2)\sigma_z} e^{-(i/\hbar)(-x/v_0)H_S}. \quad (\text{S3})$$

Going to interaction picture with respect to both system and meter Hamiltonians, the state at time  $t$  is

$$|\psi_I(t)\rangle = \exp \left[ \frac{i}{\hbar} (H_S + H_M) t \right] |\psi(t)\rangle = \int_{-\infty}^{+\infty} dx \psi_M(x) e^{(i/\hbar)(-x/v_0)H_S} e^{-i(\phi/2)\sigma_z} e^{-(i/\hbar)(-x/v_0)H_S} |x\rangle |\psi_S\rangle. \quad (\text{S4})$$

By substituting  $|\psi_S\rangle$  with its decomposition in the  $H_S$  basis and inserting the identity term  $|g_\Theta\rangle\langle g_\Theta| + |e_\Theta\rangle\langle e_\Theta|$  where needed one arrives at

$$|\psi_S, 1_\omega\rangle \rightarrow b_g I_{gg} |g_\Theta, 1_\omega\rangle + b_e I_{ee} |e_\Theta, 1_\omega\rangle + b_g I_{ge} |e_\Theta, 1_{\omega-\omega_q}\rangle + b_e I_{eg} |g_\Theta, 1_{\omega+\omega_q}\rangle, \quad (\text{S5})$$

where

$$\begin{aligned} I_{gg} &= I_{ee}^* = \langle g_\Theta | e^{-i(\phi/2)\sigma_z} | g_\Theta \rangle = \cos(\phi/2) + i \cos(\Theta) \sin(\phi/2), \\ I_{ge} &= I_{eg} = \langle g_\Theta | e^{-i(\phi/2)\sigma_z} | e_\Theta \rangle = i \sin(\Theta) \sin(\phi/2), \end{aligned} \quad (\text{S6})$$

and we have

$$\begin{aligned} |1_\omega\rangle &= \int_{-\infty}^{+\infty} dx \psi_M(x) |x\rangle = \int_{-\infty}^{+\infty} dp \tilde{\psi}_M(p) |p\rangle, \quad \text{where} \quad \tilde{\psi}(p) = \frac{1}{\sqrt{2\pi\hbar}} \int_{-\infty}^{+\infty} dx \psi_M(x) e^{-ixp/\hbar}, \\ |1_{\omega+\omega_q}\rangle &= \int_{-\infty}^{+\infty} dx \psi_M(x) e^{+i\frac{\omega_q}{v_0}x} |x\rangle = \int_{-\infty}^{+\infty} dp \tilde{\psi}_M \left( p - \frac{\hbar\omega_q}{v_0} \right) |p\rangle, \\ |1_{\omega-\omega_q}\rangle &= \int_{-\infty}^{+\infty} dx \psi_M(x) e^{-i\frac{\omega_q}{v_0}x} |x\rangle = \int_{-\infty}^{+\infty} dp \tilde{\psi}_M \left( p + \frac{\hbar\omega_q}{v_0} \right) |p\rangle. \end{aligned} \quad (\text{S7})$$

The above equations imply the frequency shifts reported in the main text as one can write  $p = (\hbar/v_0)\omega$ .

---

<sup>5</sup> See the Supplemental Material of Ref. [24] for more details.

## COMPUTATION OF OZAWA'S ERROR QUANTIFIER

Here, we compute the error of the measurement associated to the setup described in the main text. To do this we have to compute the quantity  $\varepsilon^2(|\psi_S\rangle) = \langle \psi_S, \psi_M | N^2 | \psi_S, \psi_M \rangle$  defined in the main text, where  $N = U^\dagger O_M U - O_S$ . We also recall that  $O_S = \sigma_z$  is the system observable we want to measure and  $O_M = \hat{n}_A - \hat{n}_B$ , which is also an observable, represents the measurement we perform on the meter to perform an indirect measurement on the system, while  $U$  is the unitary operator governing the entire dynamics. Finally,  $|\psi_S\rangle$  is the initial state of system  $S$  and  $|\psi_M\rangle$  is the initial state of the meter. Notice that, in general, this error depends on the initial state of the system we want to measure. However, we will show that this quantity is independent of the state  $|\psi_S\rangle$  of the qubit in our setup.

First, since there is just one meter particle, we get that  $\hat{n}_A + \hat{n}_B = \mathbb{I}$ , so that we can write that

$$UN |g_z, \psi_M\rangle = 2\hat{n}_A U |g_z, \psi_M\rangle, \quad UN |e_z, \psi_M\rangle = -2\hat{n}_B U |e_z, \psi_M\rangle. \quad (\text{S8})$$

It follows that, writing  $|\psi_S\rangle = c_g |g_z\rangle + c_e |e_z\rangle$ , we get

$$\varepsilon^2(|\psi_S\rangle) = \langle \psi_S, \psi_M | NU^\dagger UN | \psi_S, \psi_M \rangle = 4|c_g|^2 \langle g_z, \psi_M | U^\dagger \hat{n}_A U | g_z, \psi_M \rangle + 4|c_e|^2 \langle e_z, \psi_M | U^\dagger \hat{n}_B U | e_z, \psi_M \rangle. \quad (\text{S9})$$

We now have to calculate these quantities.

The total output state can be computed using Eq. (3) of the main text<sup>6</sup> and remembering the role of the two beamsplitters<sup>7</sup> and the phase shifter in arm B of the Mach-Zehnder interferometer. We get

$$U |\psi_S, \psi_M\rangle = \frac{1}{2} \left\{ |g_\Theta\rangle [b_g I_{gg} (|1_\omega, 0\rangle + |0, 1_\omega\rangle) + b_e I_{eg} (|1_{\omega+\omega_q}, 0\rangle + |0, 1_{\omega+\omega_q}\rangle) - ib_g (|1_\omega, 0\rangle - |0, 1_\omega\rangle)] + |e_\Theta\rangle [b_e I_{ee} (|1_\omega, 0\rangle + |0, 1_\omega\rangle) + b_g I_{ge} (|1_{\omega-\omega_q}, 0\rangle + |0, 1_{\omega-\omega_q}\rangle) - ib_e (|1_\omega, 0\rangle - |0, 1_\omega\rangle)] \right\}, \quad (\text{S10})$$

where the unitary operator  $U$  is the interaction picture evolution operator. The above equations imply that (with an abuse of notation<sup>8</sup> to lighten the notation)

$$\begin{aligned} \hat{n}_A U |\psi_S, \psi_M\rangle &= \frac{1}{2} \left\{ |g_\Theta\rangle [b_g I_{gg} |1_\omega\rangle + b_e I_{eg} |1_{\omega+\omega_q}\rangle - ib_g |1_\omega\rangle] + |e_\Theta\rangle [b_e I_{ee} |1_\omega\rangle + b_g I_{ge} |1_{\omega-\omega_q}\rangle - ib_e |1_\omega\rangle] \right\}, \\ \hat{n}_B U |\psi_S, \psi_M\rangle &= \frac{1}{2} \left\{ |g_\Theta\rangle [b_g I_{gg} |1_\omega\rangle + b_e I_{eg} |1_{\omega+\omega_q}\rangle + ib_g |1_\omega\rangle] + |e_\Theta\rangle [b_e I_{ee} |1_\omega\rangle + b_g I_{ge} |1_{\omega-\omega_q}\rangle + ib_e |1_\omega\rangle] \right\}. \end{aligned} \quad (\text{S11})$$

We can now compute<sup>9</sup>

$$\langle \psi_S, \psi_M | U^\dagger \hat{n}_A U | \psi_S, \psi_M \rangle = \frac{1}{4} \left\{ 1 + |I_{gg}|^2 + |I_{eg}|^2 + 2 \operatorname{Re} \left\{ -i \left( |b_g|^2 I_{gg}^* + |b_e|^2 I_{gg} \right) + 2i I_{eg} \operatorname{Re} \{ b_g^* b_e \langle 1_\omega | 1_{\omega+\omega_q} \rangle \} \right\} \right\}, \quad (\text{S12})$$

and

$$\langle \psi_S, \psi_M | U^\dagger \hat{n}_B U | \psi_S, \psi_M \rangle = \frac{1}{4} \left\{ 1 + |I_{gg}|^2 + |I_{eg}|^2 - 2 \operatorname{Re} \left\{ -i \left( |b_g|^2 I_{gg}^* + |b_e|^2 I_{gg} \right) + 2i I_{eg} \operatorname{Re} \{ b_g^* b_e \langle 1_\omega | 1_{\omega+\omega_q} \rangle \} \right\} \right\}, \quad (\text{S13})$$

where we used the fact that  $|b_g|^2 + |b_e|^2 = 1$ ,  $I_{gg} = I_{ee}^*$ ,  $I_{ge} = I_{eg}$ ,  $I_{ge}^* = -I_{eg}$ , and  $\langle 1_{\omega-\omega_q} | 1_\omega \rangle = \langle 1_\omega | 1_{\omega+\omega_q} \rangle$ .

<sup>6</sup> Even though Eq. (3) of the main text is given in interaction picture, it can be used for this calculation because  $\hat{n}_A$  and  $\hat{n}_B$  commute with the qubit's bare Hamiltonian and their value only depends on being in arm A or B and not on the actual position of the meter wavepacket.

<sup>7</sup> We consider a beamsplitter to act as follows:  $|1, 0\rangle \rightarrow$

$(1/\sqrt{2}) [|1, 0\rangle + |0, 1\rangle]$  and  $|0, 1\rangle \rightarrow (1/\sqrt{2}) [|1, 0\rangle - |0, 1\rangle]$ .

<sup>8</sup> In the following equations the particle is now localized in the arm correspondent to the applied operator,  $\hat{n}_A$  or  $\hat{n}_B$  so that we do not make explicit where the particle is for each given state as it is obvious. For example, in the equation for  $\hat{n}_B U |\psi_S, \psi_M\rangle$  the state  $|1_\omega\rangle$  stands for  $|0, 1_\omega\rangle$ .

<sup>9</sup> We recall that  $\hat{n}_A = \hat{n}_A^2$  and  $\hat{n}_B = \hat{n}_B^2$ .



Finally, we can find the averages related to  $U|g_z, \psi_M\rangle$  and  $U|e_z, \psi_M\rangle$  by making the substitutions:

$$\begin{aligned} |\psi_S\rangle &= |g_z\rangle & \text{when } b_g &\rightarrow \cos(\Theta/2), b_e \rightarrow \sin(\Theta/2); \\ |\psi_S\rangle &= |e_z\rangle & \text{when } b_g &\rightarrow -\sin(\Theta/2), b_e \rightarrow \cos(\Theta/2). \end{aligned} \quad (\text{S14})$$

Therefore, we get

$$\langle g_z, \psi_M | U^\dagger \hat{n}_A U | g_z, \psi_M \rangle = \langle e_z, \psi_M | U^\dagger \hat{n}_B U | e_z, \psi_M \rangle = \frac{1}{2} \left\{ 1 - \sin(\phi/2) [\cos^2(\Theta) + \text{Re}\{\langle 1_\omega | 1_{\omega+\omega_q} \rangle\} \sin^2(\Theta)] \right\}, \quad (\text{S15})$$

which, inserted in Eq. (S9) leads to Eq. (5) of the main text. We can see that the error being independent of the qubit's initial state is a direct consequence of the equality of the two terms in Eq. (S9).

### RATIO BETWEEN ERROR AND BOUNDS FOR DIFFERENT WAVEPACKETS

In this section, we study the ratio  $\varepsilon/\varepsilon_B$  for different wavepacket shapes: a Gaussian wavepacket  $\psi_G(x)$ , a square pulse wavepacket  $\psi_{\text{Sq}}(x)$ , and an exponential decay wavepacket  $\psi_{\text{Exp}}(x)$ . In order to make the notation less cumbersome we define the time variable  $t = -x/v_0$ . To simplify the formulas, we take Gaussian and square pulse wavepackets to be centered around  $t = 0$ . Regarding the square and exponential wavepackets, their discontinuity causes problems in the calculation of  $\Delta\omega^2$ . For this reason we use instead smooth wavefunctions which approximate them. We write

$$\psi_G(t) = \frac{\exp\left[-\frac{t^2}{4\sigma_t^2}\right]}{(2\pi)^{1/4}\sqrt{\sigma_t}}, \quad \psi_{\text{Sq}}(t) = \sqrt{\frac{\tanh\left(\frac{t+s}{\epsilon s}\right) - \tanh\left(\frac{t-s}{\epsilon s}\right)}{4s}}, \quad \psi_{\text{Exp}}(t) = \sqrt{\frac{2\gamma}{\pi\epsilon} \sin\left(\frac{\pi\epsilon}{2}\right) \left[\frac{1 + \tanh(\gamma t/\epsilon)}{2}\right]} e^{-\gamma t} \quad (\text{S16})$$

where  $2s$  indicates, more or less, the temporal length of the square wavepacket while  $\gamma$  is the decay rate of the exponential decay wavepacket. The square pulse and exponential decay wavepackets assume their idealized form in the limit  $\epsilon \rightarrow 0^+$ , but we will see that in this case their frequency variance diverges. Therefore, we will have to choose a finite value for the a-dimensional quantity  $\epsilon$ . As written, all wavepackets are normalized for any value of  $\epsilon < 1$ .

Calculating the time and frequency dispersions for the three wavepackets we get

$$\begin{aligned} \Delta t_G &= \sigma_t, & \Delta t_{\text{Sq}} &= \frac{\sqrt{4 + \pi^2 \epsilon^2}}{2\sqrt{3}} s, & \Delta t_{\text{Exp}} &= \frac{\pi\epsilon}{2\gamma \sin(\pi\epsilon/2)}, \\ \Delta\omega_G &= \frac{1}{2\sigma_t}, & \Delta\omega_{\text{Sq}} &= \frac{\sqrt{\epsilon \sinh(4/\epsilon) - 4}}{2\sqrt{2} \sinh(2/\epsilon)\epsilon s}, & \Delta\omega_{\text{Exp}} &= \sqrt{\frac{2-\epsilon}{8\epsilon}} \gamma. \end{aligned} \quad (\text{S17})$$

We can observe how the frequency dispersion of the square pulse and exponential decay wavepackets diverge for  $\epsilon \rightarrow 0$  while their time dispersion does not.

Since we are interested in the effect that using different wavepackets shapes has on the ratio  $\varepsilon/\varepsilon_B$  we consider the error as always computed for the optimal value  $\phi = \pi$  so that we get [cf. Eq. (6) and Eq. (8) of the main text]<sup>10</sup>

$$\frac{\varepsilon|_{\phi=\pi}}{\varepsilon_B} = \sqrt{2 \left(1 + 4 \frac{\Delta\omega^2}{\omega_q^2}\right)} (1 - P), \quad \text{where } P = \int_{-\infty}^{+\infty} dt |\psi_0(t)|^2 \cos(\omega_q(t + \tau)), \quad (\text{S18})$$

where  $\tau$  represents our liberty of choosing the initial position of the wavepacket. We will always choose  $\tau$  in order to maximize  $P$ . Calculating  $P$  for the three different cases gives

$$\begin{aligned} P_G &= \max_{\tau} \left\{ \cos(\omega_q \tau) \exp\left(-\frac{1}{2}\omega_q^2 \sigma_t^2\right) \right\} = \exp\left(-\frac{1}{2}\omega_q^2 \sigma_t^2\right), \\ P_{\text{Sq}} &= \max_{\tau} \left\{ \frac{\epsilon}{4} \cos(\omega_q \tau) (B_1 + B_2 + B_3 + B_4) \right\} = \frac{\epsilon}{4} |B_1 + B_2 + B_3 + B_4| \\ P_{\text{Exp}} &= \frac{\sin(\pi\epsilon/2)}{4} \max_{\tau} \left\{ e^{-i\omega_q \tau} \left[ \cot\left(\frac{\pi\epsilon(\gamma + i\omega_q)}{4\gamma}\right) \right] + \tan\left(\frac{\pi\epsilon(\gamma + i\omega_q)}{4\gamma}\right) + 2e^{2i\omega_q \tau} \csc\left(\frac{\pi\epsilon(\gamma - i\omega_q)}{2\gamma}\right) \right\}. \end{aligned} \quad (\text{S19})$$

<sup>10</sup> Eq. (6) is  $\varepsilon = \sin(\Theta)\sqrt{2(1-P)}$  while Eq. (8) is  $\varepsilon_B = \frac{\sin(\Theta)}{\sqrt{1+4(\Delta\omega/\omega_q)^2}}$ .

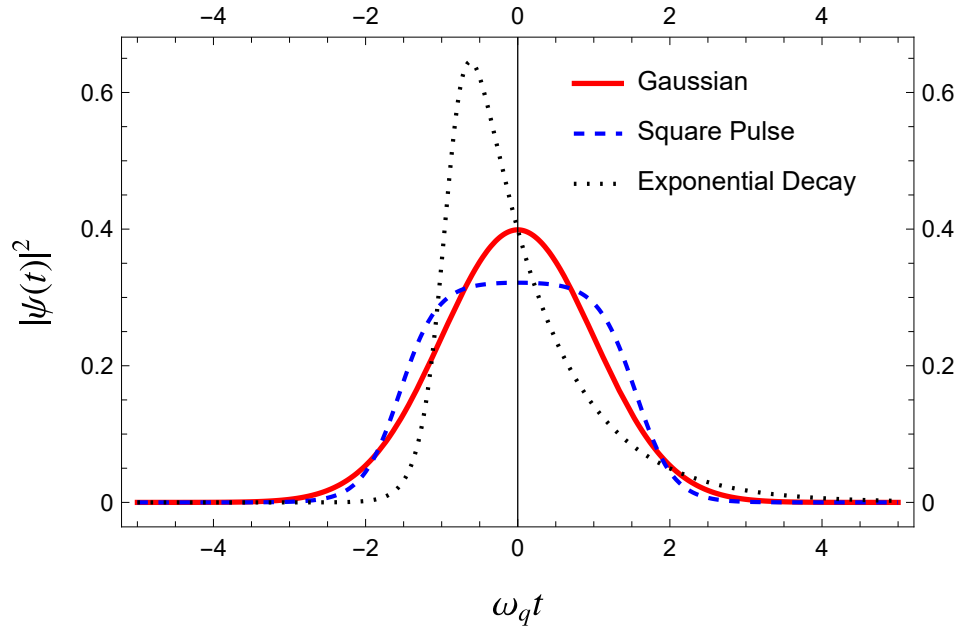


FIG. S1. Shape of  $|\psi_G(t)|^2$ ,  $|\psi_{Sq}(t)|^2$ , and  $|\psi_{Exp}(t)|^2$  for  $\epsilon = 1/\pi$  and  $\omega_q \Delta t = 1$ . All curves are plotted so that they are centered around zero. We can see how already for this value of  $\epsilon$  we get shapes resembling an ideal square pulse and an ideal exponential decay.

where

$$\begin{aligned}
 B_1 &= e^{-i\omega_q s} e^{-(\pi/2)\epsilon\omega_q s} \int_0^{-e^{-2/\epsilon}} \frac{k^{+(1/2)i\epsilon\omega_q s}}{1-k} dk, & B_2 &= e^{+i\omega_q s} e^{+(\pi/2)\epsilon\omega_q s} \int_0^{-e^{-2/\epsilon}} \frac{k^{-(1/2)i\epsilon\omega_q s}}{1-k} dk, \\
 B_3 &= e^{+i\omega_q s} e^{-(\pi/2)\epsilon\omega_q s} \int_0^{-e^{2/\epsilon}} \frac{k^{+(1/2)i\epsilon\omega_q s}}{1-k} dk, & B_4 &= e^{-i\omega_q s} e^{+(\pi/2)\epsilon\omega_q s} \int_0^{-e^{2/\epsilon}} \frac{k^{-(1/2)i\epsilon\omega_q s}}{1-k} dk.
 \end{aligned} \tag{S20}$$

In the case of the exponential decay wavepacket, the maximization over  $\tau$  does not seem possible to be made analytically, so we will do it numerically.

Now we have all the ingredients to compute the error ratio as a function of the single a-dimensional parameter  $\omega_q \Delta t$ . In every formula we substitute  $s$  and  $\gamma$  by inverting the correspondent time-dispersion equations in (S17). Then we also write the frequency dispersions as functions of  $\Delta t$ . Regarding  $\epsilon$ , we choose it to be equal to  $1/\pi$ . As one can see in fig. S1, this value already allows for a good approximation of the ideal shapes while maintaining a finite  $\Delta\omega$ . The resulting plot is the one reported in the main text.